Eur. Phys. J. B **9**, 179–182 (1999)

THE EUROPEAN PHYSICAL JOURNAL B

EDP Sciences

Rapid Note

Vibrations at 3C-SiC(001)-(3 × 2) surfaces

H. Nienhaus[a], V. van Elsbergen, and W. Mönch

Laboratorium für Festkörperphysik, Gerhard-Mercator-Universität Duisburg, 47048 Duisburg, Germany

Received 18 January 1999

Abstract. Si-terminated 3C-SiC(001) surfaces with (3×2) and (2×1) reconstructions were investigated by high-resolution electron energy-loss spectroscopy (HREELS), low-energy electron diffraction (LEED) and Auger electron spectroscopy. The surfaces were prepared by subsequent annealing steps after cleaning by heating in a Si flux. At (3×2)-reconstructed surfaces, the HREELS intensity increases while the widths of the loss lines decrease with proceeding preparation. Eventually, weak loss structures at 380 and 700 cm^{-1} are detected besides the strong Fuchs-Kliewer phonon loss peaks. They are attributed to surface-localized vibrations, *i.e.*, to stretching modes of on-top Si dimers and of C-Si-C groups, respectively. The weak features vanish after exposure to atomic deuterium, but reappear after subsequent annealing. At (2×1) reconstructed surfaces the HREELS lines are broadened and no surface-localized modes were resolved.

PACS. 68.35.Ja Surface and interface dynamics and vibrations – 79.20.-m Impact phenomena (including electron spectra and sputtering)

Within a decade, SiC has developed to a material of high technological relevance [1]. The improved quality of SiC single crystals has made outstanding electronic applications like high-temperature devices feasible and has offered a substrate for the epitaxial growth of group-III nitrides [1,2]. Likewise, the research on fundamental bulk and surface properties of SiC was initiated. Among the surfaces of the numerous modifications of SiC, the polar {001}-oriented surfaces of the cubic-structured material, 3C-SiC, have focussed much attention. For Si-terminated surfaces, a variety of (5×2), (3×2), (2×1) and c(4×2) reconstructions have been reported and investigated [3]. However, the surface structures are still not uniquely characterized to discriminate between competing models.

Here we address the (3×2) reconstruction which is formed by a Si adlayer on the ideally Si-terminated SiC(001) surface. Although extensively studied by various experimental and theoretical methods [3–13], two conflicting models of the geometric structure of 3C-SiC(001)-(3×2) surfaces are presently under discussion. Yan *et al.* proposed an *alternate dimer-row model* sketched in Figure 1a where the Si adlayer and the Si restlayer beneath are shown [4]. The adlayer atoms form tilted dimers where two dimers per (2×3) unit cell are missing. To allow a semiconducting surface the Si restlayer is expected to form dimers perpendicular to the adlayer dimers, not shown in Figure 1a. The coverage of the adlayer amounts to 1/3 of a monolayer (ML) what agrees well with experimental observations [5–7]. Recent atom-resolved scanning tunneling microscopy (STM) studies by Semond, Soukiassian *et al.* on single domain 3C-SiC(001)-(2×3) surfaces confirm this structure model [8]. In contrary, the *double dimer-row model* describes dimer rows in the Si adlayer where every third row is missing as shown in Figure 1b. It was first suggested by Dayan [9,10] and supported by STM measurements of Hara *et al.* if a buckling of the dimers is included [11]. Recent high-resolution photoemission data by Yeom

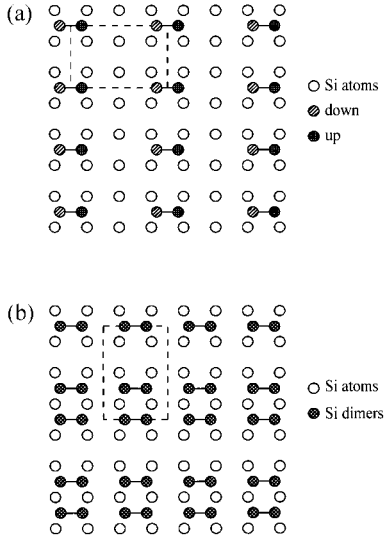

Fig. 1. Proposed atomic arrangements of 3C-SiC(001)-(3×2) surfaces; (a) *alternate dimer-row model*; (b) *double dimer-row model*.

[a] e-mail: nienhaus@uni-duisburg.de

et al. are also well explained within this model [12]. Further experimental evidence comes from low-energy electron diffraction (LEED) results concerning the (3×2) orientation relative to the (2×1)-reconstructed surface as well as the structural change from (3×2) to (3×1) after hydrogenation [3,11]. The respective coverage of the adlayer is 2/3 ML which is inconsistent with the above mentioned experimental results. The controversy may be resolved if there is a low- and a high-coverage (3×2) reconstruction depending on the preparation process and sample treatment [3]. Recently, a third model was announced but not yet published which is supposed to describe the available data consistently [13]. It is based on *ab initio* pseudopotential total energy and grand canonical potential calculations and suggests a full Si adlayer. The various studies demonstrate that much effort was focussed on the geometric and electronic structure as well as the chemical composition of 3C-SiC(001)-(3×2) surfaces. Obviously, the collected data are still not sufficient to resolve the debate.

Almost no attention has been spent on the dynamics of SiC surfaces both in experiment and theory although surface-localized vibrations are known to be closely related to structure and extremely sensitive to any surface modification. This has been successfully demonstrated for (110) surfaces of III-V compound semiconductors and for Si(001) [14,15]. So far, vibrational spectroscopy using high-resolution electron energy-loss spectroscopy (HREELS) has been applied to clean 3C-SiC surfaces to characterize strong optical Fuchs-Kliewer (FK) phonon modes [9,16,17]. However, FK phonons are completely determined by bulk properties. No microscopic surface vibration has been detected due to the large background signals and linewidths. Here, we present surface-localized vibrations at 3C-SiC(001)-(3×2) detected with HREELS after careful preparation steps.

The samples were n-doped 3C-SiC epilayers on Si with a free electron concentration of 1.4×10^{17} cm^{-3}. The surfaces were cleaned by wet chemical etching in buffered hydrofluoric acid (pH = 9) and subsequent heating in a Si atom flux under ultrahigh vacuum conditions. The procedure leaves clean 3C-SiC(001) surfaces with excess silicon on top and has been described in detail elsewhere [18]. The various reconstructions from Si- to C-rich surfaces may be obtained by annealing the samples at temperatures between 1160 and 1350 K what removes the excess Si atoms. Structure and chemical composition of the surfaces were probed with LEED and Auger electron spectroscopy (AES), respectively. HREEL spectra were recorded at primary electron energies E_p of 5 and 20 eV and in specular scattering geometry, *i.e.*, the angle of incidence ϑ_i and the angle of detection ϑ_f were equal and set to 50°. The instrumental resolution was 24 cm^{-1} (3 meV).

SiC(001)-(3×2) surfaces were prepared by careful annealing at sample temperatures T_a of 1180 ± 20 K. After a heating time of approximately 20 minutes we obtained well-defined LEED patterns showing a two-domain (3×2) structure with sharp third-order and streaky half-order spots. The streaking is a well-known phenomenon. It has been explained in terms of the *double dimer-row model* with the displacement of adjacent double dimer rows by one unit cell distance or with randomly buckled double dimer rows [10,11]. AES measurements at 3 keV electron energy gave a Si(LVV)/C(KVV) intensity ratio of 4.5 which is a typical value for Si-rich SiC surfaces [3]. Contaminants were not observed within the limits of detection.

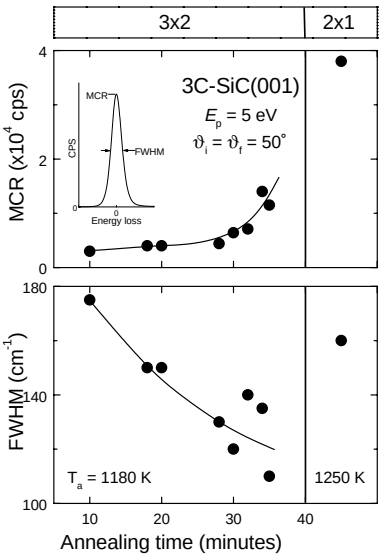

Fig. 2. Maximum count rate (MCR) and full width at half maximum (FWHM) of the elastic HREELS peak as a function of annealing time and reconstruction. The annealing temperatures T_a were 1180 K for (3×2)- and 1250 K for (2×1)-reconstructed surfaces.

As soon as clear (3×2) patterns were observed, further annealing at 1180 K did not change the LEED image significantly, but affects the surface scattering of 5 eV electrons. This is shown in Figure 2 where the maximum count rate (MCR) and the full width at half maximum (FWHM) of the HREELS peak of the elastically scattered electrons are plotted as a function of annealing time. The quantities MCR and FWHM are explained at an elastic HREELS peak in the inset of Figure 2. The results were taken from samples where annealing was interrupted for each recording of an energy-loss spectrum. The solid lines in Figure 2 are meant to guide the eye. As long as the (3×2) reconstruction is observed, MCR increases from 3000 to 12 000 counts per second (cps) and FWHM decreases from 170 to 110 cm^{-1} within the eight considered processing steps. Annealing at elevated temperature of 1250 ± 20 K removes the Si adlayer and changes the reconstruction to a two-domain (2×1) structure which is related to the Si-terminated 3C-SiC(001) surface. Here, MCR and FWHM have increased to 38 000 cps and 160 cm^{-1}, respectively.

The MCR represents the probability that incoming low-energy electrons are reflected at the surface. The mechanisms behind the reflectivity are not well understood, however, any disturbance of the periodic arrangement of the surface atoms enhances the diffuse electron scattering and reduces the number of electrons elastically scattered in specular direction. Hence, the observed

increase of MCR with every annealing step indicates a reduction of structural defects on the SiC(001)-(3 × 2) surface.

On the other hand, the FWHM of the elastic peak is closely related to low-energy surface excitations like surface plasmons of majority charge carriers [19–21]. If the excitation energy is such low that a single loss cannot be resolved, multiple excitations may broaden the spectral features. In case of surface plasmons in semiconducting materials, depletion layers due to surface band-bending lead to smaller linewidths than with flat bands. However, the observed decrease of FWHM in Figure 2 cannot be explained by a change of surface band-bending since variations of the Fermi level within the band gap were not observed at clean *n*-type 3C-SiC(001)-(3 × 2) surfaces. The Fermi level ranges between 1 and 1.2 eV above the valence-band maximum, *i.e.*, almost in midgap position [22,23]. More likely, the FWHM is related to electronic excitations in a narrow electron band of defect states at the surface. If annealing reduces the number of defect states at the surface the linewidth may decrease due to a smaller excitation probability. On the other hand, this removal of defects may not change the surface band-bending as long as there are enough charged surface states to establish the Fermi level pinning. Therefore, the observed variations of both, MCR and FWHM, indicate an improvement of the surface quality with every annealing step. Most remarkably, the (2 × 1)-reconstructed surface exhibits both a larger MCR and FWHM. This finding may be related to recent STM studies which revealed a metallic character of this surface formed above 400 °C [24]. If low-energy excitations in a surface metallic band exist for (2 × 1)-reconstructed surfaces formed at room temperature as well, HREELS features will be broadened as it is known for the Si(111)-(7 × 7) surface [20].

With decreasing linewidth of the elastic HREELS peak the spectral resolution is improved. This is demonstrated in Figure 3 showing energy-loss spectra recorded from (3 × 2)-reconstructed surfaces after annealing intervals t_a of 20, 34 and 35 minutes at 1180 K, respectively. The bottom spectrum was taken from a SiC(001)-(2 × 1) surface. As long as the linewidths are large, loss features are only observed at 935 and 1870 cm^{-1} corresponding to single and double excitations of FK phonons. After reducing the linewidths by further annealing, additional loss structures appear first at 700 ± 20 and then at 380 ± 20 cm^{-1}. They are due to microscopic surface vibrations since they are sensitive to any surface modification as shown in Figure 4. The top spectrum in Figure 4 was recorded from a 3C-SiC(001)-(3×2) surface which was annealed for 35 minutes and then exposed to atomic deuterium. D_2 molecules were dissociated at a hot tungsten filament (2100 K) and the respective molecular exposure was 100 L. After exposure, the half-order LEED spots became weaker but did not vanish completely and the FWHM increased from 110 to 150 cm^{-1}. No HREELS features other than FK phonons were detected. Heating the sample to 1200 K for two minutes recovered the original (3 × 2) reconstruction and reduced the linewidth to 100 cm^{-1} as shown at the bottom of Figure 4. Again, additional loss structures at 360 and 720 cm^{-1} were detected. Even combination losses of surface-localized vibrations and FK phonons at 1310 and 1650 cm^{-1} are resolved. A weak structure at 1535 cm^{-1} is attributed to valence vibrations of residual D atoms bound to Si.

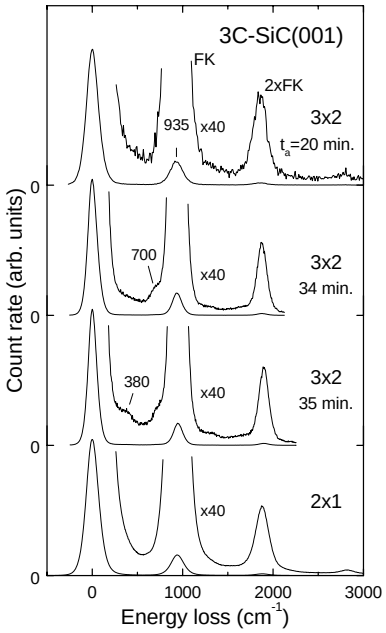

Fig. 3. HREEL spectra recorded from (3 × 2)-reconstructed surfaces after annealing times t_a of 20, 34 and 35 minutes at 1180 K, respectively, and from SiC(001)-(2 × 1). The primary electron energy was set to 5 eV.

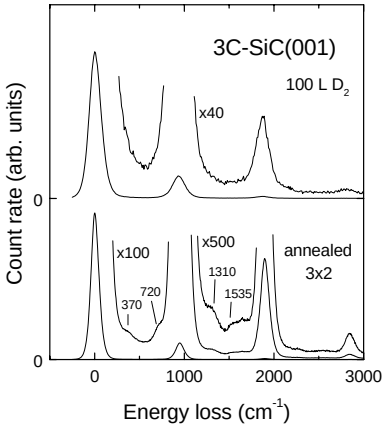

Fig. 4. Upper HREEL spectrum: SiC(001)-(3 × 2) surface exposed to atomic deuterium. The primary electron energy was set to 5 eV; lower spectrum: after annealing the exposed sample at 1200 K. The spectrum was recorded with E_p = 20 eV.

The observed surface vibrations cannot be explained by an extremely low oxygen contamination below the AES detection limit. We investigated the effect of O_2 exposure of 5 L on HREEL spectra of 3C-SiC(001)-(3 × 2) as shown at the top of Figure 3. After dosing, the background signal increased, but no decrease of linewidth or additional features were observed. Moreover, strong asymmetric stretching vibrations of oxygen adsorbed on Si would be expected

at 1090 cm^{-1} but were never observed in the SiC loss spectra [25].

Hence, the two weak loss lines are due to intrinsic vibrations in the SiC(001)-(3×2) surface. Since the HREEL spectra were taken in specular scattering geometry, the phonon energies of 380 and 700 cm^{-1} are measured in the long-wavelength limit, *i.e.*, at the center of the Brillouin zone. Here, dispersion relations are not accessible with off-specular HREELS because diffuse electron scattering is the dominant scattering mechanism even at the best prepared SiC surfaces. Although detailed calculations of the dynamics of (3×2)-reconstructed SiC(001) surfaces do not exist, molecular data and results from Si(001) surfaces may indicate the character of the vibrational modes.

Cubic SiC crystals exhibit a gap between acoustic and optical bulk phonon bands [26]. The low-energy loss at 380 cm^{-1} is within the acoustic bulk bands and represents therefore a surface resonance. The excitation energy is close to Si dimer stretching frequencies, ranging between 350 and 400 cm^{-1}, calculated for variously reconstructed Si(001) surfaces [14]. Consequently, this energy loss may be related to vibrations of the dimerized Si adatoms existing in both structure models of Figure 1. The second phonon mode at 700 cm^{-1} is located in the phonon energy gap and cannot couple to bulk phonon states. It represents a true surface-localized vibration and may be attributed to C-Si-C stretching modes in the Si restlayer. The stretching frequency is smaller than for FK phonons since for the latter longrange Coulomb interactions must be considered. Similar vibrations were found in dimethylhalosilanes by infrared and Raman spectroscopy. The A_1 mode of $SiBr_2(CH_3)_2$ with C_{2v} symmetry has an excitation energy of 682 cm^{-1} [27]. Replacing one Br atom by hydrogen results in an energy of 718 cm^{-1} for the C-Si-C stretching vibration [28]. These values are close to the observed energy at SiC(001)-(3×2) surfaces. It is likely that the frequencies of the restlayer vibrations are different for the two suggested models and that a comparison of the experimental value with calculated frequencies within the structure models may clarify structure and origin of the observed microscopic phonon modes.

In conclusion, this HREELS study reveals two weak loss structures at 380 and 700 cm^{-1} at carefully prepared 3C-SiC(001)-(3×2) surfaces. They are attributed to intrinsic surface-localized vibrations where the high-energy mode is located within the gap between acoustic and optical bulk phonon bands. The two modes may be related to stretching vibrations of on-top Si dimers and of C-Si-C groups. To identify reliably the observed losses with surface vibrations, detailed calculations of the 3C-SiC(001)-(3×2) surface dynamics are required. Together with our experimental data such theoretical results may help to resolve the conflict concerning the atomic arrangement of the surface atoms.

The support by the Deutsche Forschungsgemeinschaft under project number Mo 318/20 is gratefully acknowledged.

References

1. J.B. Casady, R.W. Johnson, Solid State Electron. **39**, 1409 (1996) and references therein.
2. M.E. Lin, S. Strite, A. Agarwal, A. Salvador, G.L. Zhou, N. Teraguchi, A. Rockett, H. Morkoç, Appl. Phys. Lett. **62**, 702 (1993).
3. V.M. Bermudez, Phys. Stat. Sol. (b) **202**, 447 (1997) and references therein.
4. H. Yan, X. Hu, H. Jónsson, Surf. Sci. **316**, 181 (1994); H. Yan, A.P. Smith, H. Jónsson, *ibid.* **330**, 265 (1995).
5. S. Hara, W.F.J. Slijkerman, J.F. van der Veen, I. Ohdomari, S. Misawa, E. Sakuma, S. Yoshida, Surf. Sci. **231**, L196 (1990).
6. T. Yoshinobu, I. Izumikawa, H. Mitsui, T. Fuyuki, H. Matsunami, Appl. Phys. Lett. **59**, 2844 (1991).
7. X. Hu, H. Yan, M. Kokyama, F.S. Ohuchi, J. Phys.-Cond. **7**, 1069 (1995).
8. F. Semond, P. Soukiassian, A. Mayne, G. Dujardin, L. Douillard, C. Jaussaud, Phys. Rev. Lett. **77**, 2013 (1996); P. Soukiassian, F. Semond, A. Mayne, G. Dujardin, *ibid.* **79**, 2498 (1997).
9. M. Dayan, J. Vac. Sci. Technol. A **3**, 361 (1985); **4**, 38 (1986); Surf. Sci. **149**, L33 (1985).
10. R. Kaplan, Surf. Sci. **215**, 111 (1989).
11. S. Hara, S. Misawa, S. Yoshida, Y. Aoyagi, Phys. Rev. B **50**, 4548 (1994); S. Hara, J. Kitamura, H. Okushi, S. Misawa, S. Yoshida, Y. Tokumaru, Surf. Sci. **357-358**, 436 (1996).
12. H.W. Yeom, Y.-C. Chao, S. Terada, S. Hara, S. Yoshida, R.I.G. Uhrberg, Phys. Rev. B **56**, R15525 (1997); H.W. Yeom, Y.-C. Chao, I. Matsuda, S. Hara, S. Yoshida, R.I.G. Uhrberg, Phys. Rev. B **58**, 10540 (1998).
13. W. Lu, P. Krüger, J. Pollmann, Phys. Rev. Lett. **81**, 2292 (1998).
14. J. Fritsch, P. Pavone, Surf. Sci. **344**, 159 (1995).
15. H. Nienhaus, Phys. Rev. B **56**, 13194 (1997).
16. H. Nienhaus, T.U. Kampen, W. Mönch, Surf. Sci. **324**, L328 (1995).
17. T. Balster, V.M. Polyakov, F.S. Tautz, H. Ibach, J.A. Schaefer, Mat. Sci. Forum **264-268**, 347 (1998).
18. V. van Elsbergen, T.U. Kampen, W. Mönch, Surf. Sci. **365**, 443 (1996).
19. J.A. Stroscio, W. Ho, Phys. Rev. Lett. **54**, 1573 (1985).
20. B.N.J. Persson, J.E. Demuth, Phys. Rev. B **30**, 5968 (1984).
21. L.H. Dubois, B.R. Zegarski, B.N.J. Persson, Phys. Rev. B **35**, 9128 (1987).
22. T.M. Parrill, Y.W. Chung, Surf. Sci. **243**, 96 (1991).
23. O. Janzen, Diploma thesis, University of Duisburg, 1996.
24. V.Y. Aristov, L. Douillard, O. Fauchoux, P. Soukiassian, Phys. Rev. Lett. **79**, 3700 (1997).
25. H. Ibach, H.D. Bruchmann, H. Wagner, Appl. Phys. A **29**, 113 (1982).
26. M. Hofmann, A. Zywietz, K. Karch, F. Bechstedt, Phys. Rev. B **50**, 13401 (1994).
27. H. Murata, S. Hayashi, J. Chem. Phys. **19**, 1217 (1951).
28. J.R. Durig, C.W. Hawley, J. Chem. Phys. **58**, 237 (1973).